Received: 18 January 2020 | Accepted: 1 August 2020

DOI: 10.1002/jcp.30010

ORIGINAL RESEARCH ARTICLE

Journal of Cellular Physiology WILEY

RPL41 sensitizes retinoblastoma cells to chemotherapeutic drugs via ATF4 degradation

Wen Geng[1] | Jiaxu Ren[1] | Huimin Shi[2] | Feng Qin[3] | Xiaohe Xu[1] | Sheng Xiao[4] | Yisheng Jiao[5] | Aiyuan Wang[1]

[1]Department of Ophthalmology, Shengjing Hospital of China Medical University, Shengyang, Liaoning, China

[2]Department of Ophthalmology, Xiangyang Central Hospital, Affiliated Hospital of Hubei University of Arts and Science, Xiangyang, Hubei, China

[3]Department of Ophthamology, Shenyang Aier Eye Hospital, Shenyang, Liaoning, China

[4]Department of Pathology, Brigham and Women's Hospital of Harvard Medical School, Boston, Massachusetts

[5]Department of Obstetrics and Gynecology, Shengjing Hospital of China Medical University, Shengyang, Liaoning, China

Correspondence
Yisheng Jiao, Department of Obstetrics and Gynecology, Shengjing Hospital of China Medical University, No. 36 Sanhao Street, Shengyang, Liaoning 110004, China.
Email: jiaoys@sj-hospital.org

Aiyuan Wang, Department of Ophthalmology, Shengjing Hospital of China Medical University, No. 36 Sanhao Street, Shengyang, Liaoning 110004, China.
Email: wangay@sj-hospital.org

Funding information
National Natural Science Foundation of China, Grant/Award Numbers: 81272873, 81372878; Guidance Plan of Natural Science Foundation from the Department of Science and Technology of Liaoning Province, Grant/Award Number: 2019-ZD-0738

Abstract

Retinoblastoma is the most common intraocular cancer with metastatic potential affecting infants and children. Although chemotherapy is available for retinoblastoma, side effects and drug resistance are frequent. *Rpl41*, encoding ribosomal protein L41 (RPL41), has been identified as a tumor suppressor gene, and its targeted degradation of activating transcription factor 4 (ATF4) produces an antitumor effect. The goal of the present study is to provide experimental evidence for the clinical application of a small peptide regimen in combination with chemotherapy for the treatment of retinoblastoma and to investigate the mechanism of their combined cytotoxicity. It was observed that treatment with the RPL41 peptide alone decreased the viability, migration, and invasion of retinoblastoma Y79 and Weri-Rb1 cells, in addition to promoting cell apoptosis and cell cycle arrest. Furthermore, RPL41 protein levels showed a significantly decreased trend in retinoblastoma specimens, whereas ATF4 protein levels tended to be increased. Mechanistically, ATF4 degradation as a result of RPL41 peptide treatment was observed in retinoblastoma Y79 and Weri-Rb1 cells. Most important, low-dose administration of the RPL41 peptide significantly enhanced the antitumor effect of carboplatin, and further analysis confirmed their synergistic effect as anti-retinoblastoma therapy, indicating that RPL41 sensitized Y79 and Weri-Rb1 retinoblastoma cells to carboplatin. Thus, our data provide a preclinical rationale for the exploration of the RPL41 peptide as a potential adjuvant to carboplatin treatment in retinoblastoma.

KEYWORDS

ATF4, carboplatin, drug resistance, retinoblastoma, RPL41

1 | INTRODUCTION

Retinoblastoma is the most common malignant intraocular tumor in infants and children (Dimaras et al., 2012). Although the primary tumor can often be successfully treated by chemotherapy and localized therapeutics, extraocular dissemination through the optic nerve or the choroid into the nervous or vascular systems represents a serious clinical complication (Asnaghi et al., 2019). Resistance to current therapies and the serious toxic effects contribute largely to the generally fatal outcome of metastatic lesions

Abbreviations: ATF4, activating transcription factor 4; CI, combination index; RPL41, ribosomal protein L41; TUNEL, TdT-mediated dUTP nick-end labeling; uPA, urokinase-type plasminogen activator; VEGF, vascular endothelial growth factor.

Wen Geng and Jiaxu Ren contributed equally to this study.

in the central nervous system or in distant organs, such as bone and bone marrow (Wong et al., 2014). Thus, there is an urgent need to elucidate novel strategies targeting retinoblastoma metastasis and drug resistance.

During tumor development, neoplastic cells are inevitably challenged by limited levels of oxygen, glucose, and amino acids (Ackerman & Simon, 2014; Wortel, van der Meer, Kilberg, & van Leeuwen, 2017). Not merely as a result of malignant transformation, molecular events induced by stress microenvironment, like unfolded protein response, can also actively promote tumor development, involving cancer metastasis, angiogenesis, and drug resistance (Wortel et al., 2017). Endoplasmic reticulum stress results from the increased demand for protein synthesis due to the activation of oncogenes and the high proliferation rate stimulating the unfolded protein response, which largely contributes to adaptive transcriptional responses and cell transformation, drug resistance, immunosuppression, angiogenesis, and metastasis (Cubillos-Ruiz, Bettigole, & Glimcher, 2017). Activating transcription factor 4 (ATF4) is well known to be induced by stress and is a common downstream effector that is frequently upregulated in cancer cells (Linares et al., 2017; Wortel et al., 2017). Besides, the vascular endothelial growth factor (VEGF) and urokinase-type plasminogen activator (uPA) play important roles in tumor progression (Kwaan & Lindholm, 2019; Madunić, 2018; Wegiel, Ekberg, Talasila, Jalili, & Persson, 2009). ATF4 has been demonstrated to bind directly to the promoter region of VEGF and uPA genes, or engage in unidirectional cross-talk with activator protein-1, leading to the increased expression of uPA, which plays an important role in tumor angiogenesis, invasion, and metastasis (Jain, Chakraborty, Raja, Kale, & Kundu, 2008; Lossos et al., 2019; Malabanan, Kanellakis, Bobik, & Khachigian, 2008). Moreover, the enhanced expression of ATF4 was also related to tumor drug resistance, which may involve autophagy induction, increased production of the antioxidant glutathione, and transactivation of STAT3 expression (Lewerenz et al., 2012; Wu et al., 2010; Zhu et al., 2014). However, the explicit role of ATF4 in retinoblastoma progression remains to be elucidated, as effective therapeutic agents targeting ATF4 are unavailable.

Ribosomal proteins (RPs) are abundant RNA-binding proteins, with more than 80 unique members present in ribosomes, the cellular translational machinery, and many carry out extraribosomal functions (Zhou, Liao, Liao, Liao, & Lu, 2015). Recent findings indicate that RPs play a crucial role in tumor progression and may be developed as promising prognostic markers and therapeutic targets (Xie, Guo, Yu, Wang, & Chen, 2018). Ribosomal protein L41 (RPL41), a small peptide consisting of 25 amino acids, has been characterized as the smallest and most basic eukaryotic protein, rich in arginine and lysine residues, and possessing no posttranslational modifications (S. Wang et al., 2010). Our previous studies have demonstrated that the antitumor roles of RPL41 are mediated by the interaction with ATF4 and cytoskeleton components (S. Wang et al., 2010; A. Wang et al., 2011); however, the relationship between RPL41 and retinoblastoma progression, in addition to the underlying mechanism, remains to be elucidated.

2 | MATERIALS AND METHODS

2.1 | Tissue samples

In total, 30 retinoblastoma tissue specimens were enrolled in the present study between 1997 and 2018 at the Shengjing Hospital of China Medical University (Shenyang, China). Clinical specimens from patients who received any treatment before surgery were excluded and all diagnoses were confirmed by pathologists in the same team. Primary retinoblastoma tissues and adjacent noncancerous tissues were used for the analysis of ATF4 and RPL41 levels. The experimental protocols were approved by the Ethics Committee of the Shengjing Hospital of China Medical University.

2.2 | RPL41 synthesis

The RPL41 peptide (NH_2-MRAKWRKKRMRRLKRKRRKMRQRSK-OH) was synthesized by GenScript (Nanjing, China), as described previously (A. Wang et al., 2011). The purity of peptide was determined to be >95% by high-performance liquid chromatography (HPLC), and it was subsequently analyzed by mass spectrometry and HPLC. The peptide was reconstituted in double-distilled water at a final concentration of 10 mM.

2.3 | Cell culture and treatment

The human retinoblastoma cell lines, Y79 and Weri-Rb1, were purchased from American Type Culture Collection (Manassas). All cells were cultured in Roswell Park Memorial Institute 1640 (RPMI-1640) medium (Sigma-Aldrich, St. Louis), supplemented with 10% fetal bovine serum (FBS; Gibco, Carlsbad) and 1% penicillin–streptomycin–glutamine (100X; Gibco), at 37°C and 5% CO_2. During the experiments, cells were exposed to an equal volume of the control or RPL41 peptide (0, 20, 40, 60, 80, and 100 μM in double-distilled water) for 24, 48, or 72 hr. To analyze the combined drug efficiency, cells were treated with carboplatin at the indicated concentrations (2.5, 5, 10, 20, 40, and 80 μM) for 24 hr, followed by the RPL41 peptide (20 μM) for a further 24 hr.

2.4 | Immunohistochemistry

The tissue paraffin blocks were prepared, sectioned at 4 μm thickness, and handled as described previously (Song et al., 2018). The sections were washed, blocked, and incubated with primary antibodies against ATF4 (diluted 1:150; Abcam, Cambridge, UK) and RPL41 (diluted 1:800; Abcam) at 4°C overnight. After washing thoroughly, the sections were incubated for 40 min at 37°C with an appropriate secondary antibody (diluted 1:200; Vector, Burlingame). Images were captured by computerized image acquisition software (NIS-Elements F3.0) and an Olympus microscope (Nikon E800).

2.5 | Cell viability assay

Cell viability was assessed using the CellTiter-Glo® luminescent cell viability assay (G7570; Promega, Beijing, China), according to the manufacturer's protocol. Briefly, Y79 and Weri-Rb1 cells (1×10^4 cells/well) were seeded on 96-well plates in triplicate. Cells were treated with the control or RPL41 peptide at the concentrations indicated above. A blank control group containing medium without cells was used to obtain background luminescence. After peptide incubation, the CellTiter-Glo® reagent was added to the medium, shaken for 2 min, and incubated with the cells for 10 min at room temperature. The half-maximal inhibitory concentration (IC_{50}) value for each formulation was calculated using GraphPad Prism 6 (GraphPad Software, Inc., San Diego).

2.6 | Cell apoptosis detection

Annexin V-APC/7-AAD and TdT-mediated dUTP nick-end labeling (TUNEL) staining were used to detect apoptotic cells, as described previously (Song et al., 2018). After treatment with the control or RPL41 peptide, as mentioned above, cell suspensions were labeled with annexin V-APC/7-AAD and subjected to flow cytometry (CytoFLEXflow; Beckman, Kraemer Boulevard, Brea, CA). For TUNEL staining, cell suspensions were incubated with 50-μl TUNEL solution for 60 min at 37°C, and then cells were washed and resuspended in phosphate-buffered saline (PBS). Cell smear was performed and observed by fluorescence microscopy (Olympus IX71; Tokyo, Japan).

2.7 | Cell cycle analysis

The Cell Cycle Detection Kit from KeyGen Biotech (Nanjing) was used according to the manufacturer's protocol. Briefly, cells were fixed with 70% ethanol at 4°C overnight. After washing twice with ice-cold PBS, cells were incubated with a working solution (RNase A 50 μg/ml and propidium iodide [PI] 50 μg/ml) for 30 min at 37°C and subsequently analyzed by flow cytometry (CytoFLEXflow; Beckman).

2.8 | Western blot analysis

Total protein was collected from cell lysates using the radioimmunoprecipitation assay buffer (Beyotime, Beijing) supplemented with protease inhibitors (Beyotime). After quantitation by the bicinchoninic acid assay, samples (40-μg protein) were subjected to 10–12% sodium dodecyl sulphate-polyacrylamide gel electrophoresis and transferred to polyvinylidene difluoride membrane (Millipore). Membranes were incubated at 4°C overnight with primary antibodies against the following proteins: cleaved caspase-3 (1:500; Affinity), VEGF-A (1:1,000; Abcam), uPA (1:1,000; Proteintech, China), ATF4 (1:1,000; Cell Signaling Technology, MA), and glyceraldehyde 3-phosphate dehydrogenase (1:10,000; Proteintech). Subsequently, the membranes were incubated with the respective horseradish peroxidase-conjugated secondary antibodies (1:2,000; Proteintech). Protein bands were detected using enhanced chemiluminescence western blot analysis substrate (Affinity).

2.9 | Migration and invasion assays

Cell migration and invasion play a key role in tumor metastasis; we investigated the effect of RPL41 peptide on these activities in retinoblastoma cells. The migration of retinoblastoma Y79 and Weri-Rb1 cells was assessed using the transwell assay with an insert chamber (8-μm pore size; Corning, NY). Briefly, after treatment with RPL41 peptide for 24 hr, equal quantities of Y79 and Weri-Rb1 cells suspended in 200-μl RPMI-1640 medium containing 1% FBS were seeded on the upper chambers, and 300-μl RPMI-1640 medium containing 20% FBS was in the lower chambers. After 12 hr of incubation at 37°C, the cells in lower chambers were collected. The viable cell was detected by trypan blue exclusion dye and counted under a microscope, which could exclude the possibility that reduction in cell migration was attributable to cell death. Also, the invasion assay was performed using similar methods as mentioned above, except that the chamber membrane was precoated with Matrigel (2.5 μg/μl). The number of cells invading across matrigel was counted.

2.10 | Immunofluorescence

After peptide treatment, as indicated above, cells were fixed with 4% paraformaldehyde, permeated with 0.1% Triton X-100 in PBS, and blocked with sheep serum. Subsequently, cells were incubated overnight with an anti-ATF4 primary antibody (1:200; Cell Signaling Technology). The next day, cells were washed thoroughly with PBST, incubated with an Alexa Fluor 488-conjugated secondary antibody (Proteintech) for 1 hr in the dark, washed again, and sealed with a mounting medium containing 4′,6-diamidino-2-phenylindole (Beyotime). Images were captured with a fluorescence microscope (Olympus IX71).

2.11 | Determination of combination index value

The synergism between RPL41 and carboplatin in inhibiting cell proliferation was analyzed by calculating the combination index (CI) values using the CompuSyn software (Chou, 2006, 2010). The experiment was designed as a nonconstant ratio combination *t*, according to the suggestion of guidebook. In the experiments above, we found that RPL41 could obviously degrade ATF4 at a low dose of 20 μM without significant cell death. On the basis of this finding, WERI-RB1and Y79 cells were treated with 20 μM RPL41 and several concentrations of carboplatin, and the cell viability was determined by the method described in Section 2.5 and analyzed by the CompuSyn software, which follows the median effect principle to identify

the CI value. The CI index furnishes a value that quantitatively indicates synergism (CI < 1), additive effect (CI = 1), and antagonism (CI > 1).

2.12 | Statistical analysis

Data were analyzed using the SPSS software (17.0; IBM, IL), and they are presented as the mean ± standard deviation of at least three independent experiments performed in triplicate. Student's *t* test and one- or two-way analysis of variance were used for the analysis, and $p < .05$ was considered statistically significant.

3 | RESULTS

3.1 | RPL41 exerts anti-retinoblastoma activity on Y79 and Weri-Rb1 cells

To assess the antioncogenic role of RPL41 in retinoblastoma, the RPL41 peptide was synthesized, as described previously (A. Wang et al., 2011), and its effect on the viability of human retinoblastoma Y79 and Weri-Rb1 cells was examined. As shown in Figure 1, cells were incubated with increasing concentrations of the RPL41 peptide (20, 40, 60, 80, and 100 μM) for 24, 48, or 72 hr. The results of catalytic fluorescein reaction reveal that RPL41 peptide treatment significantly reduced the viability of Y79 and Weri-Rb1 cells in a time- and concentration-dependent manner in comparison with the control peptide (Figure 1). The IC_{50} values of the RPL41 peptide for Y79 and Weri-Rb1 cells were 52.37 and 72.22 μM after a 24-hr treatment, and 43.53 and 52.89 μM after a 48-hr treatment, respectively. After treatment for 72 hr, the IC_{50} values of the RPL41 peptide were 38.21 and 39.68 μM, respectively.

3.2 | RPL41 promotes apoptosis of Y79 and Weri-Rb1 cells

To investigate the anti-retinoblastoma mechanism of the RPL41 peptide, the apoptotic events in human retinoblastoma Y79 and Weri-Rb1 cell lines were examined. After treatment with the RPL41 or control peptide for 24 hr at the indicated concentrations, flow cytometry was employed to detect apoptotic cells. As shown in Figure 2a,b, the apoptosis rates of Y79 and Weri-Rb1 cells were significantly increased by RPL41 peptide treatment as compared to those following treatment with the control peptide, which occurred in a concentration-dependent manner. Moreover, the characteristic morphological features of apoptotic cells were examined by TUNEL staining. A greater number of DNA strand breaks were observed in cells treated with the RPL41 peptide in comparison with the control peptide (Figure 2c,d), indicating the increased occurrence of apoptosis. Furthermore, the level of the apoptotic marker protein, cleaved caspase-3, was examined by the western blot analysis. As shown in Figure 2e,f, increased cleaved caspase-3 levels confirmed enhanced apoptotic events in cells treated with the RPL41 peptide, whereas the control peptide induced no significant changes in

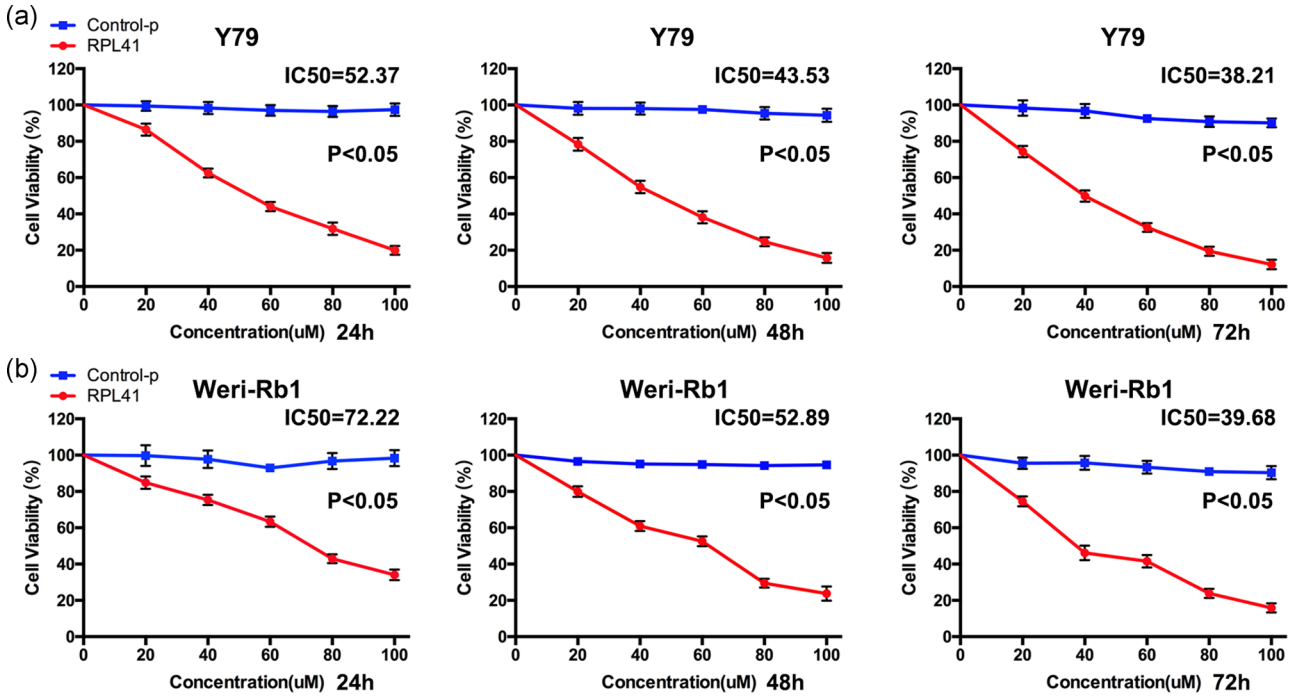

FIGURE 1 The RPL41 peptide reduces the viability of retinoblastoma cell lines. Increasing concentrations of the RPL41 or control peptides were used to treat (a) Y79 or (b) Weri-Rb1 cells for 24, 48, or 72 hr, which were subsequently harvested for viability evaluation. Data are expressed as the mean ± standard deviation ($n = 3$). IC_{50}, half maximal inhibitory concentration; RPL41, ribosomal protein L41

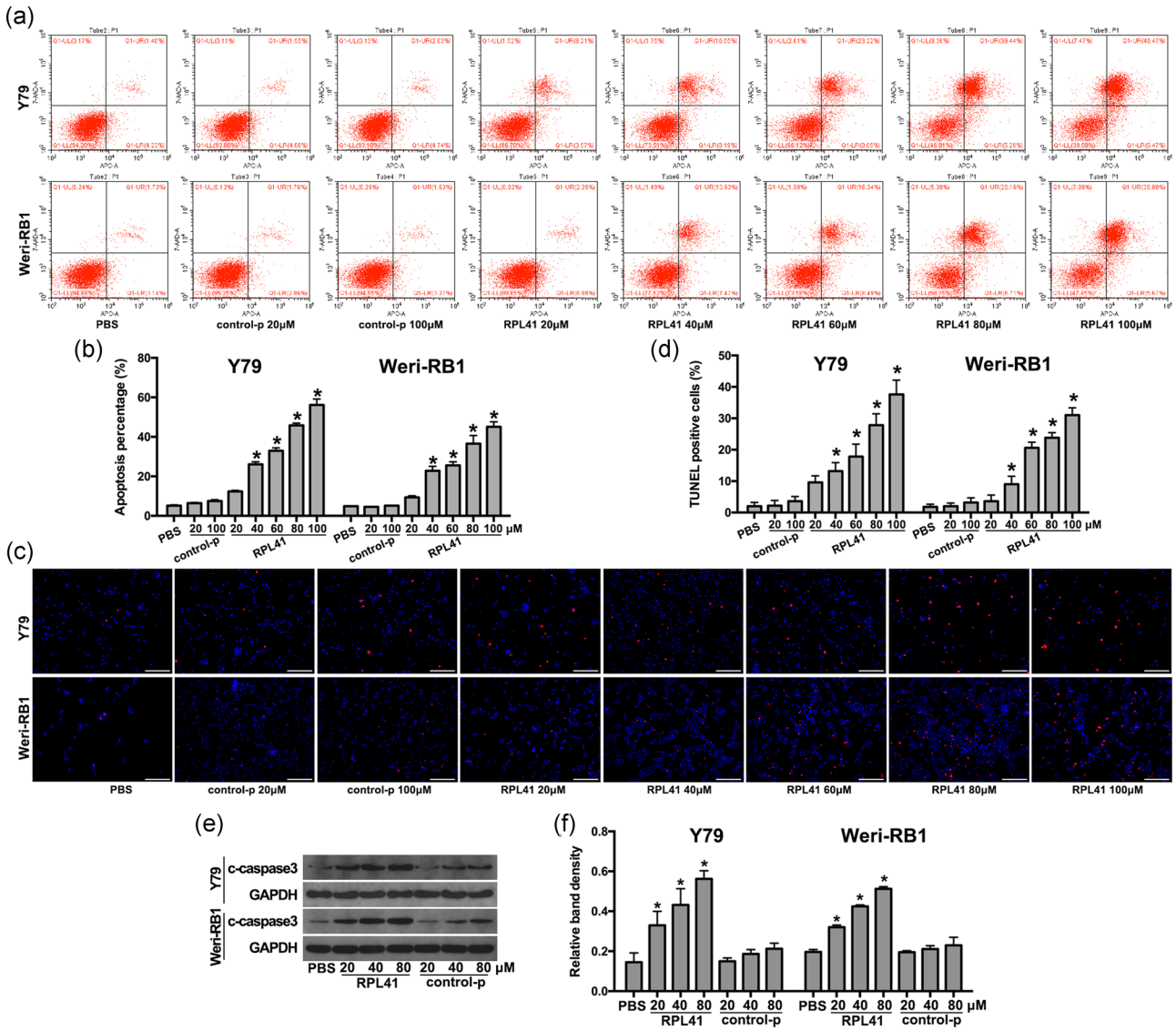

FIGURE 2 The RPL41 peptide induces apoptotic events in retinoblastoma cell lines. Y79 and Weri-Rb1 retinoblastoma cells were exposed to PBS, the control peptide (20 and 100 μM), or the RPL41 peptide (20, 40, 60, 80, and 100 μM) for 48 hr. Apoptosis was detected by annexin V-APC/7-AAD and TUNEL staining using flow cytometry and fluorescence microscopy, respectively. (a and b) Representative scatter plots for annexin V-APC/7-AAD staining and quantitative analysis of the apoptosis percentage. The proportion of live cells (third quadrant), apoptotic cells (first and fourth quadrants), and necrotic cells (second quadrant) was measured. $^*p < .05$ versus PBS (24 hr). (c and d) Representative fluorescent images and quantitative analysis of TUNEL-positive cells. $^*p < .05$ versus PBS (24 hr). (e and f) Representative western blot and quantitation of the level of cleaved caspase-3. $^*p < .05$ versus PBS (24 hr). Data are expressed as the mean ± standard deviation ($n = 3$). Scale bar = 100 μm (b). GAPDH, glyceraldehyde 3-phosphate dehydrogenase; PBS, phosphate-buffered saline; RPL41, ribosomal protein L41; TUNEL, TdT-mediated dUTP nick-end labeling

these protein levels. Collectively, these findings indicate that the increased level of apoptosis contributed to the anti-retinoblastoma effect of RPL41.

3.3 | RPL41 induces G1-phase cell cycle arrest in Y79 and Weri-Rb1 cells

To determine whether cell cycle arrest is involved in RPL41-mediated anti-retinoblastoma activity, cell cycle distribution was analyzed by PI staining using flow cytometry. The analysis of the cellular DNA content reveals that the percentage of cells in the G1 phase increased in a concentration-dependent manner from 59.06% to 82.48% in Y79 cells and from 42.72% to 54.27% in Weri-Rb1 cells after treatment with 20–100-μM RPL41 peptide (Figure 3). Similarly, there was a decrease in the percentage of cells in the S phase. Interestingly, the effect of RPL41 on cell cycle arrest was more significant in Y79 cells. Taken together, these results suggest that the RPL41 peptide induced cell cycle arrest at the G1 phase in Y79 and Weri-Rb1 cells.

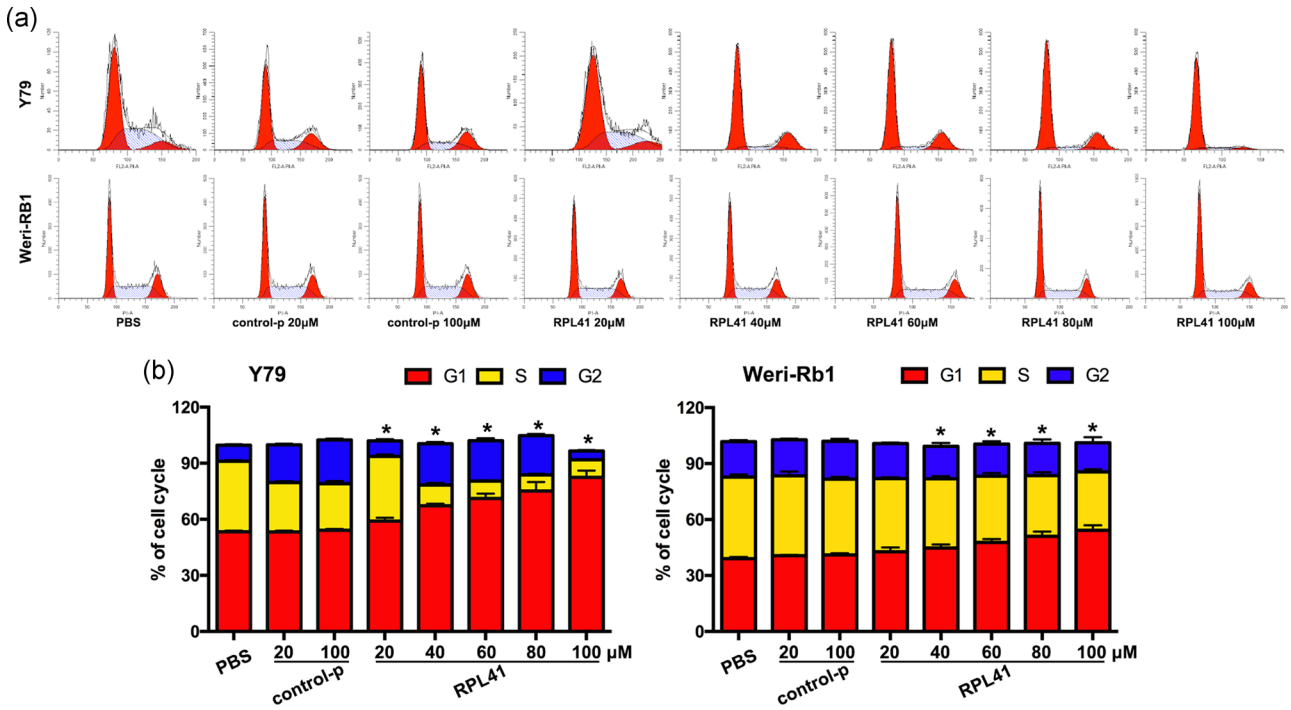

FIGURE 3 The RPL41 peptide induces G1-phase cell cycle arrest of retinoblastoma cell lines. (a) Y79 and Weri-Rb1 retinoblastoma cells were exposed to PBS, the control peptide (20 and 100 μM), or the RPL41 peptide (20, 40, 60, 80, and 100 μM) for 24 hr. The cell cycle was evaluated by PI staining using flow cytometry. (b) The percentages of cell cycle distribution at G1, S, and G2 phases were analyzed. *$p < .05$ versus PBS (24 hr). Data are expressed as the mean ± standard deviation ($n = 3$). PBS, phosphate-buffered saline; PI, propidium iodide; RPL41, ribosomal protein L41

3.4 | RPL41 suppresses migration and invasion of Y79 and Weri-Rb1 cells

The transwell assay was employed to evaluate the migration and invasion activity of Y79 and Weri-Rb1 cells. The viable cells crossing over the chamber membrane were counted. In the migration assay, the results showed that the number of Y79 and Weri-Rb1 cells in the lower chamber was significantly decreased by RPL41 peptide treatment (Figure 4a,b). Similarly, the results of invasion assay also showed that RPL41 peptide treatment could significant decrease the number of Y79 and Weri-Rb1 cells in the lower chamber (Figure 4c,d). Furthermore, the VEGF and uPA, which play roles in the promotion of tumor cell migration and invasion (Conn et al., 2009; Ryan et al., 2006), were examined. Western blot analysis results show that the protein levels of VEGF and uPA were both significantly decreased after RPL41 peptide treatment (Figure 4e–h). These results indicated that RPL41 peptide had a negative impact on the migration and invasion of Y79 and Weri-Rb1 cells.

3.5 | RPL41-meditated anti-retinoblastoma activity involves ATF4 degradation

As a stress-induced transcription factor, ATF4 facilitates cellular responses to unfavorable conditions and is closely related to tumor progression (Wortel et al., 2017). According to our previous studies, ATF4 degradation is induced by RPL41 after treatment in several tumor cell lines; therefore, we further confirmed its role in RPL41-meditated anti-retinoblastoma activity in the present study. First, we assessed the protein levels of ATF4 and RPL41 in human retinoblastoma tissue specimens. As shown, the rates of positive ATF4 staining in retinoblastoma specimens were 56.1–95.6% (mean 76.1%), which were much higher than those in adjacent normal retinal tissue (6.8–19.6%; mean 13.4%; Figure 5a). Moreover, a significant difference in ATF4 protein expression was observed between differentiated and undifferentiated tumor specimens. As shown, undifferentiated tumors presented a higher rate of ATF4 positive staining (79.7–95.6%; mean 87.3%) as compared with that of differentiated tumors (56.1–75.1%; mean 64.9%). Conversely, RPL41 protein levels were higher in adjacent normal retinal tissues (75.6–88.0%; mean 81.2%) as compared to those in differentiated (38.7–53.3%; mean 46.7%) and undifferentiated (2.9–8.5%; mean 6.4%) tumor specimens (Figure 5b).

To further determine whether RPL41 can induce ATF4 degradation in human retinoblastoma cell lines, Y79 and Weri-Rb1 cells were treated with the RPL41 or control peptide for 24 hr at the indicated concentrations, after which the ATF4 protein levels were examined. Western blot analysis results show that RPL41 peptide treatment decreased the ATF4 protein level as compared to that following treatment with the control peptide or PBS in both Y79

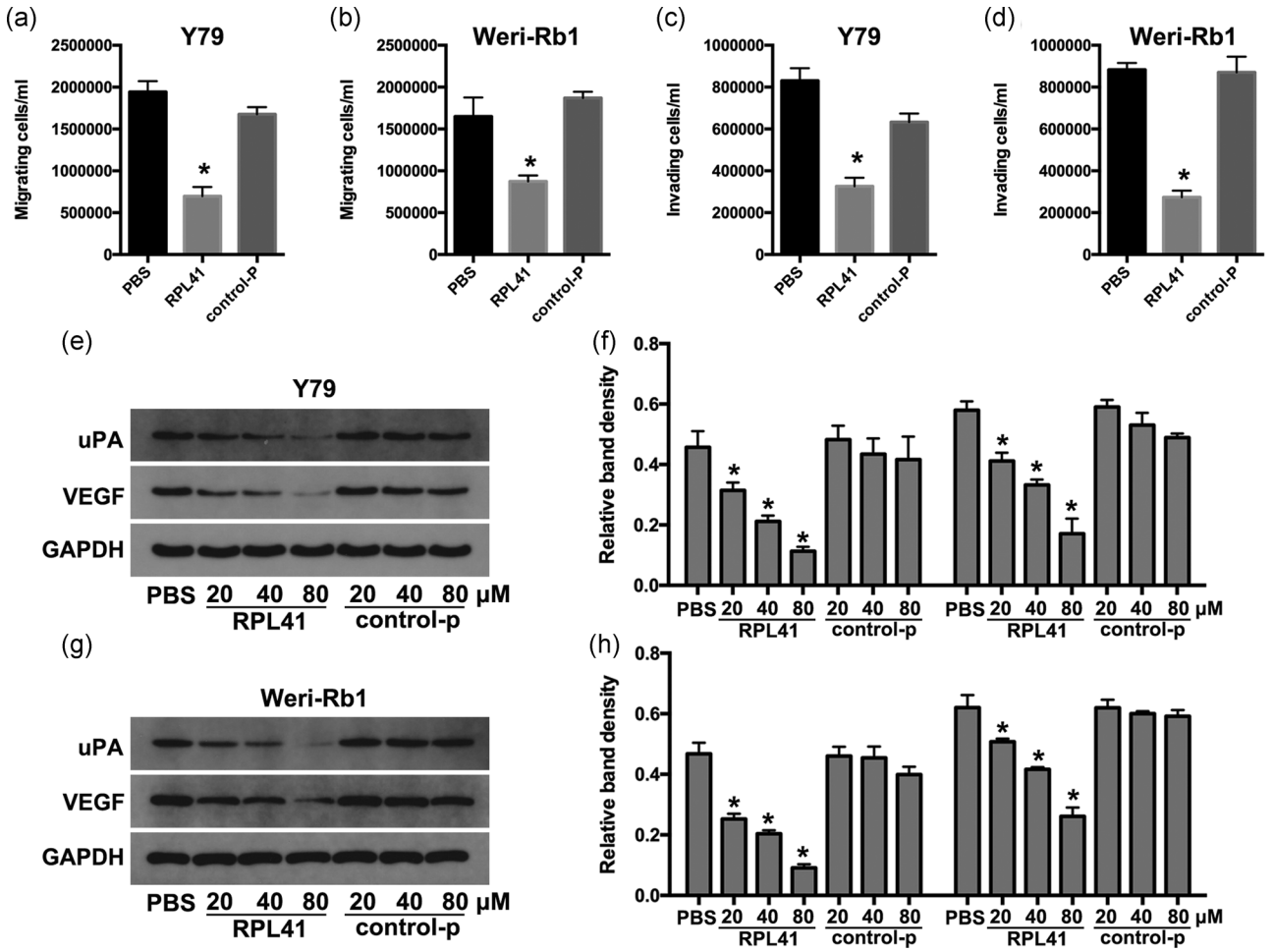

FIGURE 4 The RPL41 peptide inhibits the migration and invasion activity of retinoblastoma cell lines. (a–d) Y79 and Weri-Rb1 retinoblastoma cells were exposed to PBS, the control peptide (80 μM), or the RPL41 peptide (80 μM) for 24 hr. The secondary transwell assay was performed. The migrating cell number of (a) Y79 and (b) Weri-Rb1 in the lower chamber was counted. The invading cell number of (c) Y79 and (d) Weri-Rb1 in lower chamber was counted. *$p < .05$ versus PBS (24 hr). (e–h) Y79 and Weri-Rb1 retinoblastoma cells were exposed to PBS, the control peptide (20, 40, and 80 μM), or the RPL41 peptide (20, 40, and 80 μM) for 24 hr. The protein expression levels of uPA and VEGF were evaluated by the western blot analysis in (e and f) Y79 and (g and h) Weri-Rb1 cells. *$p < .05$ versus PBS (24 hr). Data are expressed as the mean ± standard deviation ($n = 3$). GAPDH, glyceraldehyde 3-phosphate dehydrogenase; PBS, phosphate-buffered saline; RPL41, ribosomal protein L41; uPA, urokinase-type plasminogen activator; VEGF, vascular endothelial growth factor

(Figure 6a) and Weri-Rb1 (Figure 6b) cells. Similarly, immunofluorescence staining of ATF4 confirmed that the RPL41 peptide induced its degradation in Y79 and Weri-Rb1 cells (Figure 6c,d).

3.6 | The RPL41 peptide significantly sensitizes Y79 and Weri-Rb1 cells to the chemotherapy agent, carboplatin

Although carboplatin is relatively efficiently used as systemic chemotherapy in retinoblastoma, the effective drug concentration can cause unwanted side effects, such as bone marrow suppression, ototoxicity, and renal toxicity (Dimaras et al., 2012; Y. F. Wang et al., 2013). Thus, the RPL41 peptide was evaluated as a potential sensitizer of Y79 and Weri-Rb1 cells to carboplatin. A fixed dose of 20-μM RPL41 peptide was used with increasing concentrations of carboplatin in a viability assay. As shown in Figures 7a and 7e, the cell survival curve reveals that Y79 and Weri-Rb1 cells were sensitized to carboplatin after treatment with the RPL41 peptide. The synergy between the RPL41 peptide and carboplatin in Y79 and Weri-Rb1 cells was examined by the CI analysis (Figure 7).

4 | DISCUSSION

Retinoblastoma is the most common intraocular malignancy in the developing retina during childhood. Although chemotherapy is recommended as the most important therapeutic modality and results in a good prognosis in some patients (Shields, Manjandavida, Lally et al., 2014), drug resistance and adverse effects have largely

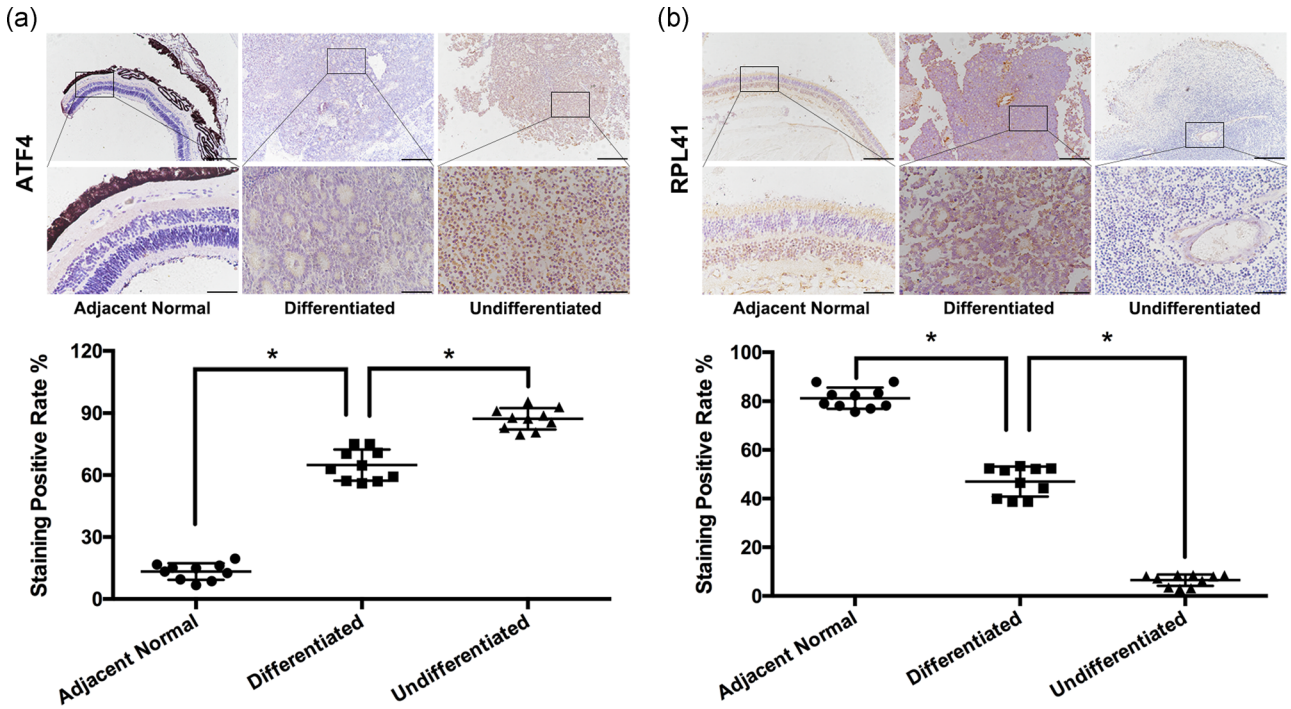

FIGURE 5 ATF4 and RPL41 protein levels were examined in 30 retinoblastoma specimens. (a) Representative immunohistochemical images showing ATF4 labeling and quantitation of the positive staining percentage. *$p < .05$. (b) Representative immunohistochemical images showing RPL41 labeling and quantitation of the positive staining percentage. *$p < .05$. Scale bar = 50 μm (upper); scale bar = 200 μm (lower). ATF4, activating transcription factor 4; RPL41, ribosomal protein L41

contributed to the compromised therapeutic efficacy in current clinical administration (He, Lee, & Kim, 2018). Many regimens have been explored for the development of novel therapeutic approaches or the improvement of current therapies, such as immunotherapy, nanoparticles, and naturally occurring plant-derived flavonoids (Liu et al., 2013; Qu, Meng, Yu, & Wang, 2017; Zou & Xu, 2018). Here, we identified the roles of the antitumor gene, *rpl41*, and its druggable molecular target, ATF4, in the regulation of cell growth, invasion, and drug resistance in Y79 and Weri-Rb1 retinoblastoma cells. RPL41 peptide treatment decreased the viability, migration, and invasion of Y79 and Weri-Rb1 cells, in addition to promoting apoptosis and cell cycle arrest. Further study shows that ATF4 degradation was involved in the RPL41-induced anti-retinoblastoma mechanism.

Irrespective of their essential roles in ribosome assembly and protein translation, multiple ribosomal proteins possess extra-ribosomal functions that are closely related to tumor initiation, inflammatory response, and neurodegenerative diseases (Cruz-Rivera et al., 2018; Doherty et al., 2010; Zhou et al., 2015). *Rpl41* has been identified as a tumor suppressor gene, and its deficiency, down-regulation, or mutations have been detected in tumors (A. Wang et al., 2011). As our previous studies have identified an antitumor role for RPL41 in several tumor cell lines (S. Wang et al., 2010; A. Wang et al., 2011), the present study was conducted to further confirm its significant inhibitory effect on retinoblastoma cells. We found that cell viability of retinoblastoma Y79 and Weri-Rb1 cells was significantly suppressed by treatment with the RPL41 peptide, and apoptosis and cell cycle arrest were induced. In addition, RPL41 protein levels decreased with retinoblastoma progression. These results suggest that the RPL41 peptide exerted antioncogenic effects on retinoblastoma cells.

The migration and invasion activities of tumor cells contribute largely to tumor progression and metastasis. In our present study, we found that RPL41 peptide treatment significantly suppressed migration and invasion activities of retinoblastoma Y79 and Weri-Rb1 cells. Besides the well-known roles in inducing angiogenesis and remodeling extracellular matrix (ECM), VEGF and uPA have been reported to directly participate in mediating cell migration and invasion. Depletion of intracellular VEGF in multiple colorectal cancer cell lines led to a strong inhibition of their migration and invasion, and the administration of exogenous VEGF could enhance the U-937 leukemic cell migration and invasion (Bhattacharya et al., 2017; Wegiel et al., 2009). Similarly, uPA with its receptor uPAR formed a complex with vitronectin and integrins, which enhanced tumor cells to adhere to the ECM and promoted tumor cell metastasis. Furthermore, RNA interference-mediated downregulation of uPA could reduce meningioma cell invasion and migration (Kondraganti et al., 2006; Kwaan & Lindholm, 2019). Thus, we examined the VEGF and uPA levels in RPL41 peptide-treated retinoblastoma cells as the cell migration and invasion markers. Expectedly, RPL41 peptide treatment could significantly decrease the VEGF and uPA protein levels, which further indicates its antioncogenic role in retinoblastoma cells.

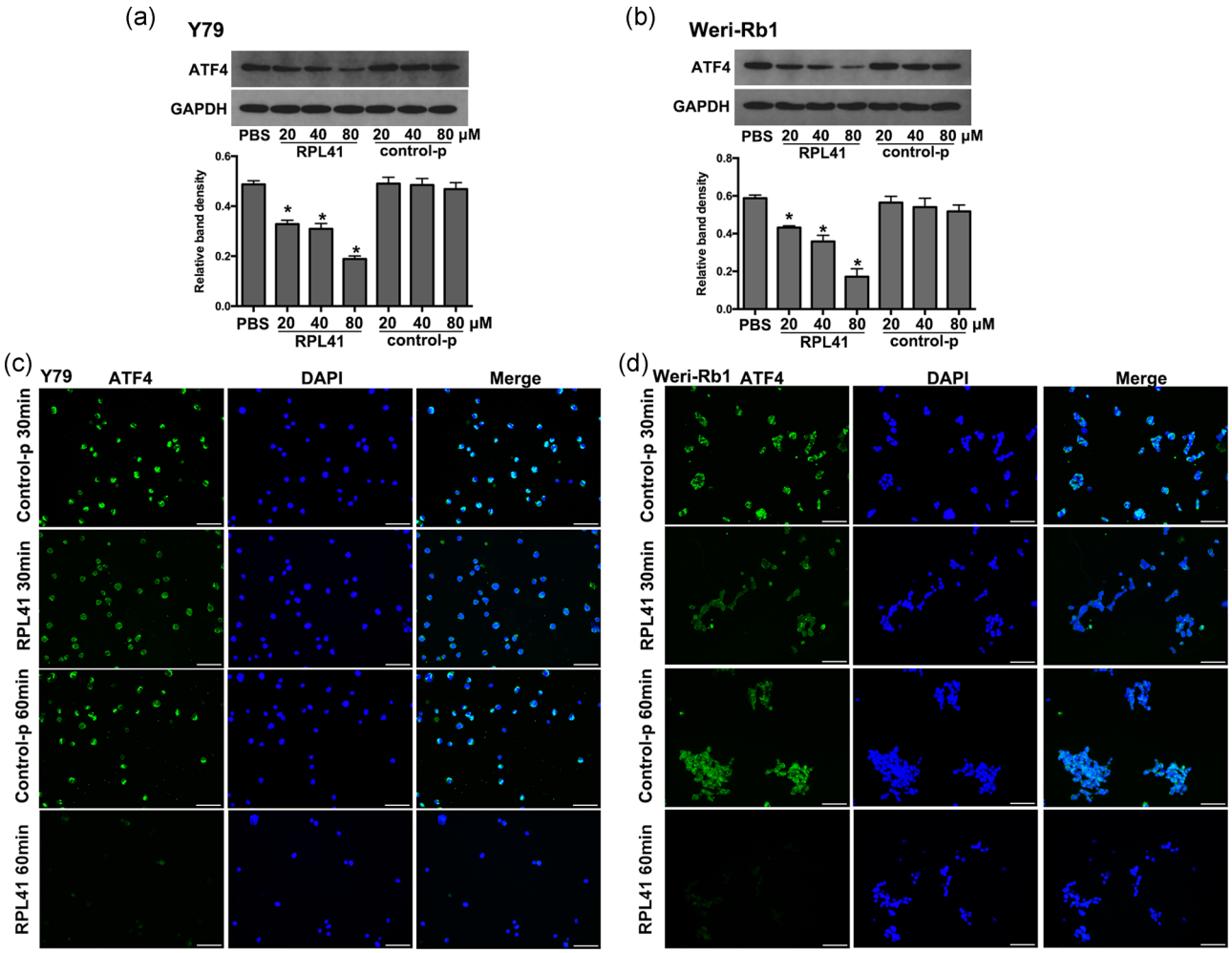

FIGURE 6 The RPL41 peptide promotes ATF4 degradation in retinoblastoma cell lines. (a and b) Y79 and Weri-Rb1 retinoblastoma cells were exposed to PBS, the control peptide (20, 40, and 80 μM), or the RPL41 peptide (20, 40, and 80 μM) for 24 hr. The protein expression levels of ATF4 were evaluated by the western blot analysis in (a) Y79 and (b) Weri-Rb1 cells. $^{*}p < .05$ versus PBS (24 hr). Data are expressed as the mean ± standard deviation ($n = 3$). (c and d) Y79 and Weri-Rb1 retinoblastoma cells were exposed to the control peptide (20 μM) or the RPL41 peptide (20 μM) for 30 or 60 min. The ATF4 levels were detected by immunofluorescence staining. Scale bar = 50 μm. ATF4, activating transcription factor 4; DAPI, 4′,6-diamidino-2-phenylindole; GAPDH, glyceraldehyde 3-phosphate dehydrogenase; PBS, phosphate-buffered saline; RPL41, ribosomal protein L41

Owing to the development of high-throughput sequencing technology, several tumor-related genes have been identified in the human genome (Zhang et al., 2018). Gene therapy and various gene delivery systems have been introduced; however, these strategies are accompanied by potential risks, largely due to their clinical transformation, such as infection, immunogenic response, or low expression efficiency (Blanquer, Grijpma, & Poot, 2015). As observed in previous studies, synthesized peptides can be used to target the precise protein domain and perform local injection, which greatly enhances the accuracy and efficiency of clinical application (Geng, Qin, Ren, Xiao, & Wang, 2018; Li et al., 2018). In the present study, the synthesized RPL41 peptide was used, which is analogous to the product of the tumor suppressor gene, *Rpl41*, and its exogenous application inhibited retinoblastoma cell growth.

The ability of cancer cells to adapt to extrinsic and intrinsic stresses is critical for maintaining viability and growth. ATF4-mediated gene transcripts are involved in antioxidant responses, autophagy, and amino acid biosynthesis and transport, which are essential for the stress response of cancer cells (Dey et al., 2015; Wortel et al., 2017). Thus, we examined ATF4 protein expression levels in retinoblastoma specimens and observed a significant increase as compared to normal tissues. RPL41 has been demonstrated to induce ATF4 phosphorylation at serine 219, further promoting ATF4 degradation by the proteasome (A. Wang et al., 2011). Therefore, we further explored whether ATF4 degradation is involved in the anti-retinoblastoma mechanism exerted by RPL41. In the present study, in vitro experiments using the RPL41 peptide confirmed that the RPL41 peptide induced ATF4 degradation in Y79 and Weri-Rb1 retinoblastoma cells. These findings indicate that the increase in ATF4 expression was associated with retinoblastoma progression and that the RPL41 peptide exerted its anti-retinoblastoma effect by inducing ATF4 degradation.

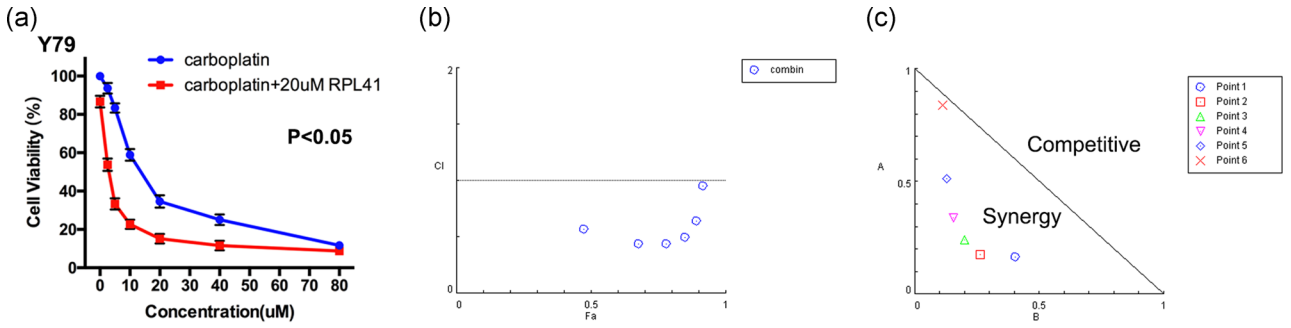

(d)

Carboplatin Dose (μM)	Rpl41 Dose (μM)	Effect	CI
Point1	2.5	20	0.475	0.56776
Point2	5	20	0.677	0.43909
Point3	10	20	0.779	0.44196
Point4	20	20	0.851	0.49472
Point5	40	20	0.893	0.64018
Point6	80	20	0.916	0.95198

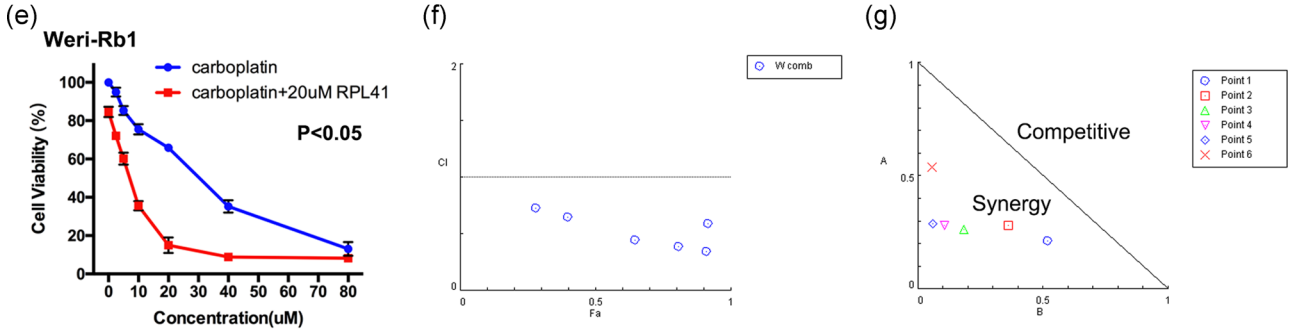

(h)

Carboplatin Dose (μM)	Rpl41 Dose (μM)	Effect	CI
Point1	2.5	20	0.279	0.73085
Point2	5	20	0.399	0.64525
Point3	10	20	0.647	0.44813
Point4	20	20	0.807	0.38977
Point5	40	20	0.911	0.34717
Point6	80	20	0.918	0.59386

FIGURE 7 The RPL41 peptide sensitizes retinoblastoma cell lines to carboplatin. Y79 and Weri-Rb1 retinoblastoma cells were exposed to increasing concentrations of carboplatin (2.5, 5, 10, 20, 40, and 80 μM) for 24 hr, followed by the RPL41 peptide (20 μM) for further 24 hr. (a–d) Cell viability assay (a), Fa–CI plot (b), and normalized isobologram (c) representing synergy between carboplatin and the RPL41 peptide, and the CI values for the combination of carboplatin and the RPL41 peptide (d) were analyzed in Y79 retinoblastoma cells. (e–h) Cell viability assay (e), Fa–CI plot (f), and normalized isobologram (g) representing synergy between carboplatin and the RPL41 peptide, and the CI values for the combination of carboplatin and the RPL41 peptide (h) were analyzed in Weri-Rb1 retinoblastoma cells. CI, combination index; RPL41, ribosomal protein L41

Due to the essential application of chemotherapy for the treatment of retinoblastoma, despite the existence of secondary drug resistance and adverse effects, many studies have focused on the identification of novel genetic or molecular targets whose disruption may sensitize retinoblastoma cells to current standard chemotherapy regimens (He et al., 2018; Mitra et al., 2011). The ATF4 pathway serves as an attractive therapeutic target, whose manipulation can alleviate drug resistance in tumor cells (S. Wang et al., 2010; A. Wang et al., 2011; Zhu et al., 2014). On the basis of our findings that ATF4 was upregulated in retinoblastoma specimens and RPL41 peptide treatment-induced ATF4 degradation, we further investigated the combined use of the RPL41 peptide and the conventional anti-retinoblastoma drug, carboplatin, in retinoblastoma cell lines. It was found that RPL41 sensitized Y79 and Weri-Rb1 retinoblastoma cells to carboplatin treatment, indicating a synergistic mechanism.

In addition, there were some limitations to this study. In the cell cycle analysis, the effect of RPL41 on cell cycle arrest was more significant in Y79 cells when compared to WERI-Rb1, even at the highest dose. This may be related to the invasiveness of the tumor. In the future studies, we would perform further experiments on the more aggressive retinoblastoma cell lines such as RB355 and NCC-Rb51 cell lines. Moreover, we administrated the RPL41 peptide by

intravitreal injection in our previous study and found that the intravitreal injection of RPL41 peptide could efficiently suppress neovascularization in mice retina (Geng et al., 2018). Besides, intravitreal administration of chemotherapeutic agents has been recommended to be effective (Shields, Manjandavida, Arepalli et al., 2014). However, the intraocular stage is required for intravitreal injection and it is difficult to observe and master the tumor growth in retinoblastoma model of mice intravitreal transplantation. A proper animal model of retinoblastoma will provide more direct evidence to reveal the therapeutic efficiency of RPL41 peptide.

5 | CONCLUSION

In conclusion, we demonstrate that the RPL41 peptide suppressed retinoblastoma cell viability, migration, and invasion, and induced apoptosis and cell cycle arrest through the promotion of ATF4 degradation. Moreover, low-dose administration of the RPL41 peptide sensitized retinoblastoma cells to carboplatin treatment. Further experimental and preclinical investigations of the RPL41 peptide and its anti-ATF4 potential should be performed to develop this promising anti-retinoblastoma therapy.

ACKNOWLEDGMENTS

This study was supported by the National Natural Science Foundation of China (Grant Numbers 81372878 and 81272873) and the Guidance Plan of Natural Science Foundation from the Department of Science and Technology of Liaoning Province (Grant Number 2019-ZD-0738).

CONFLICT OF INTERESTS

The authors declare that there are no conflict of interests.

AUTHOR CONTRIBUTIONS

W. G., A. W., and Y. J. performed the research design. W. G., J. R., X. X., and F. Q. conducted the experiments. S. X. designed and provided the RPL41. W. G., H. S., and A. W. wrote the manuscript.

DATA AVAILABILITY STATEMENT

The datasets used and/or analyzed during the current study are available from the corresponding authors on reasonable request.

ETHICS STATEMENT

The collection of human specimens was approved by the Ethics Committee of the Shengjing Hospital of China Medical University.

ORCID

Wen Geng http://orcid.org/0000-0001-7702-6629
Jiaxu Ren http://orcid.org/0000-0001-6821-9218
Huimin Shi http://orcid.org/0000-0002-0744-6529
Feng Qin http://orcid.org/0000-0002-4396-557X
Xiaohe Xu http://orcid.org/0000-0001-8761-0511
Sheng Xiao http://orcid.org/0000-0002-1566-9386
Yisheng Jiao http://orcid.org/0000-0002-5896-7447
Aiyuan Wang http://orcid.org/0000-0001-7239-8159

REFERENCES

Ackerman, D., & Simon, M. C. (2014). Hypoxia, lipids, and cancer: Surviving the harsh tumor microenvironment. *Trends in Cell Biology*, *24*(8), 472–478.

Asnaghi, L., White, D. T., Key, N., Choi, J., Mahale, A., Alkatan, H., … Eberhart, C. G. (2019). ACVR1C/SMAD2 signaling promotes invasion and growth in retinoblastoma. *Oncogene*, *38*(12), 2056–2075.

Bhattacharya, R., Fan, F., Wang, R., Ye, X., Xia, L., Boulbes, D., & Ellis, L. M. (2017). Intracrine VEGF signalling mediates colorectal cancer cell migration and invasion. *British Journal of Cancer*, *117*(6), 848–855.

Blanquer, S. B., Grijpma, D. W., & Poot, A. A. (2015). Delivery systems for the treatment of degenerated intervertebral discs. *Advanced Drug Delivery Reviews*, *84*, 172–187.

Chou, T. C. (2006). Theoretical basis, experimental design, and computerized simulation of synergism and antagonism in drug combination studies. *Pharmacological Reviews*, *58*(3), 621–681.

Chou, T. C. (2010). Drug combination studies and their synergy quantification using the Chou-Talalay method. *Cancer Research*, *70*(2), 440–446.

Conn, E. M., Botkjaer, K. A., Kupriyanova, T. A., Andreasen, P. A., Deryugina, E. I., & Quigley, J. P. (2009). Comparative analysis of metastasis variants derived from human prostate carcinoma cells: Roles in intravasation of VEGF-mediated angiogenesis and uPA-mediated invasion. *American Journal of Pathology*, *175*(4), 1638–1652.

Cruz-Rivera, Y. E., Perez-Morales, J., Santiago, Y. M., Gonzalez, V. M., Morales, L., Cabrera-Rios, M., & Isaza, C. E. (2018). A selection of important genes and their correlated behavior in Alzheimer's disease. *Journal of Alzheimer's Disease*, *65*(1), 193–205.

Cubillos-Ruiz, J. R., Bettigole, S. E., & Glimcher, L. H. (2017). Tumorigenic and immunosuppressive effects of endoplasmic reticulum stress in cancer. *Cell*, *168*(4), 692–706.

Dey, S., Sayers, C. M., Verginadis, I. I., Lehman, S. L., Cheng, Y., Cerniglia, G. J., … Koumenis, C. (2015). ATF4-dependent induction of heme oxygenase 1 prevents anoikis and promotes metastasis. *The Journal of Clinical Investigation*, *125*(7), 2592–2608.

Dimaras, H., Kimani, K., Dimba, E. A., Gronsdahl, P., White, A., Chan, H. S., & Gallie, B. L. (2012). Retinoblastoma. *Lancet*, *379*(9824), 1436–1446.

Doherty, L., Sheen, M. R., Vlachos, A., Choesmel, V., O'Donohue, M. F., Clinton, C., … Gazda, H. T. (2010). Ribosomal protein genes RPS10 and RPS26 are commonly mutated in Diamond-Blackfan anemia. *American Journal of Human Genetics*, *86*(2), 222–228.

Geng, W., Qin, F., Ren, J., Xiao, S., & Wang, A. (2018). Mini-peptide RPL41 attenuated retinal neovascularization by inducing degradation of ATF4 in oxygen-induced retinopathy mice. *Experimental Cell Research*, *369*(2), 243–250.

He, H., Lee, C., & Kim, J. K. (2018). UHRF1 depletion sensitizes retinoblastoma cells to chemotherapeutic drugs via downregulation of XRCC4. *Cell Death & Disease*, *9*(2), 164.

Jain, S., Chakraborty, G., Raja, R., Kale, S., & Kundu, G. C. (2008). Prostaglandin E2 regulates tumor angiogenesis in prostate cancer. *Cancer Research*, *68*(19), 7750–7759.

Kondraganti, S., Gondi, C. S., McCutcheon, I., Dinh, D. H., Gujrati, M., Rao, J. S., & Olivero, W. C. (2006). RNAi-mediated downregulation of urokinase plasminogen activator and its receptor in human meningioma cells inhibits tumor invasion and growth. *International Journal of Oncology*, *28*(6), 1353–1360.

Kwaan, H. C., & Lindholm, P. F. (2019). Fibrin and fibrinolysis in cancer. *Seminars in Thrombosis and Hemostasis*, *45*(4), 413–422.

Lewerenz, J., Sato, H., Albrecht, P., Henke, N., Noack, R., Methner, A., & Maher, P. (2012). Mutation of ATF4 mediates resistance of neuronal cell lines against oxidative stress by inducing xCT expression. *Cell Death and Differentiation*, *19*(5), 847–858.

Li, D., Song, H., Mei, H., Fang, E., Wang, X., Yang, F., … Tong, Q. (2018). Armadillo repeat containing 12 promotes neuroblastoma progression through interaction with retinoblastoma binding protein 4. *Nature Communications*, *9*(1), 2829.

Linares, J. F., Cordes, T., Duran, A., Reina-Campos, M., Valencia, T., Ahn, C. S., … Diaz-Meco, M. T. (2017). ATF4-induced metabolic reprograming is a synthetic vulnerability of the p62-deficient tumor stroma. *Cell Metabolism*, *26*(6), 817–829.e816.

Liu, Q., Wang, Y., Wang, H., Liu, Y., Liu, T., & Kunda, P. E. (2013). Tandem therapy for retinoblastoma: Immunotherapy and chemotherapy enhance cytotoxicity on retinoblastoma by increasing apoptosis. *Journal of Cancer Research and Clinical Oncology*, *139*(8), 1357–1372.

Lossos, C., Liu, Y., Kolb, K. E., Christie, A. L., van Scoyk, A., Prakadan, S. M., … Weinstock, D. M. (2019). Mechanisms of lymphoma clearance induced by high-dose alkylating agents. *Cancer Discovery*, *9*, 944–961.

Madunić, J. (2018). The urokinase plasminogen activator system in human cancers: An overview of its prognostic and predictive role. *Thrombosis and Haemostasis*, *118*(12), 2020–2036.

Malabanan, K. P., Kanellakis, P., Bobik, A., & Khachigian, L. M. (2008). Activation transcription factor-4 induced by fibroblast growth factor-2 regulates vascular endothelial growth factor-A transcription in vascular smooth muscle cells and mediates intimal thickening in rat arteries following balloon injury. *Circulation Research*, *103*(4), 378–387.

Mitra, M., Kandalam, M., Sundaram, C. S., Verma, R. S., Maheswari, U. K., Swaminathan, S., & Krishnakumar, S. (2011). Reversal of stathmin-mediated microtubule destabilization sensitizes retinoblastoma cells to a low dose of antimicrotubule agents: A novel synergistic therapeutic intervention. *Investigative Ophthalmology & Visual Science*, *52*(8), 5441–5448.

Qu, W., Meng, B., Yu, Y., & Wang, S. (2017). EpCAM antibody-conjugated mesoporous silica nanoparticles to enhance the anticancer efficacy of carboplatin in retinoblastoma. *Materials Science & Engineering. C, Materials for Biological Applications*, *76*, 646–651.

Ryan, B. M., Konecny, G. E., Kahlert, S., Wang, H. J., Untch, M., Meng, G., … Duffy, M. J. (2006). Survivin expression in breast cancer predicts clinical outcome and is associated with HER2, VEGF, urokinase plasminogen activator and PAI-1. *Annals of Oncology*, *17*(4), 597–604.

Shields, C. L., Manjandavida, F. P., Arepalli, S., Kaliki, S., Lally, S. E., & Shields, J. A. (2014). Intravitreal melphalan for persistent or recurrent retinoblastoma vitreous seeds: Preliminary results. *JAMA ophthalmology*, *132*(3), 319–325.

Shields, C. L., Manjandavida, F. P., Lally, S. E., Pieretti, G., Arepalli, S. A., Caywood, E. H., … Shields, J. A. (2014). Intra-arterial chemotherapy for retinoblastoma in 70 eyes: Outcomes based on the international classification of retinoblastoma. *Ophthalmology*, *121*(7), 1453–1460.

Song, Y., Li, S., Geng, W., Luo, R., Liu, W., Tu, J., … Yang, C. (2018). Sirtuin 3-dependent mitochondrial redox homeostasis protects against AGEs-induced intervertebral disc degeneration. *Redox Biology*, *19*, 339–353.

Wang, S., Huang, J., He, J., Wang, A., Xu, S., Huang, S. F., & Xiao, S. (2010). RPL41, a small ribosomal peptide deregulated in tumors, is essential for mitosis and centrosome integrity. *Neoplasia*, *12*(3), 284–293.

Wang, Y. F., Kunda, P. E., Lin, J. W., Wang, H., Chen, X. M., Liu, Q. L., & Liu, T. (2013). Cytokine-induced killer cells co-cultured with complete tumor antigen-loaded dendritic cells, have enhanced selective cytotoxicity on carboplatin-resistant retinoblastoma cells. *Oncology Reports*, *29*(5), 1841–1850.

Wang, A., Xu, S., Zhang, X., He, J., Yan, D., Yang, Z., & Xiao, S. (2011). Ribosomal protein RPL41 induces rapid degradation of ATF4, a transcription factor critical for tumour cell survival in stress. *Journal of Pathology*, *225*(2), 285–292.

Wegiel, B., Ekberg, J., Talasila, K. M., Jalili, S., & Persson, J. L. (2009). The role of VEGF and a functional link between VEGF and p27Kip1 in acute myeloid leukemia. *Leukemia*, *23*(2), 251–261.

Wong, J. R., Morton, L. M., Tucker, M. A., Abramson, D. H., Seddon, J. M., Sampson, J. N., & Kleinerman, R. A. (2014). Risk of subsequent malignant neoplasms in long-term hereditary retinoblastoma survivors after chemotherapy and radiotherapy. *Journal of Clinical Oncology*, *32*(29), 3284–3290.

Wortel, I. M. N., van der Meer, L. T., Kilberg, M. S., & van Leeuwen, F. N. (2017). Surviving stress: Modulation of ATF4-mediated stress responses in normal and malignant cells. *Trends in Endocrinology and Metabolism*, *28*(11), 794–806.

Wu, W. K., Sakamoto, K. M., Milani, M., Aldana-Masankgay, G., Fan, D., Wu, K., … Sung, J. J. (2010). Macroautophagy modulates cellular response to proteasome inhibitors in cancer therapy. *Drug Resistance Updates*, *13*(3), 87–92.

Xie, X., Guo, P., Yu, H., Wang, Y., & Chen, G. (2018). Ribosomal proteins: Insight into molecular roles and functions in hepatocellular carcinoma. *Oncogene*, *37*(3), 277–285.

Zhang, P., Xia, J. H., Zhu, J., Gao, P., Tian, Y. J., Du, M., … Wang, L. (2018). High-throughput screening of prostate cancer risk loci by single nucleotide polymorphisms sequencing. *Nature Communications*, *9*(1), 2022.

Zhou, X., Liao, W. J., Liao, J. M., Liao, P., & Lu, H. (2015). Ribosomal proteins: Functions beyond the ribosome. *Journal of Molecular Cell Biology*, *7*(2), 92–104.

Zhu, H., Chen, X., Chen, B., Chen, B., Fan, J., Song, W., … Zhao, Y. (2014). Activating transcription factor 4 mediates a multidrug resistance phenotype of esophageal squamous cell carcinoma cells through transactivation of STAT3 expression. *Cancer Letters*, *354*(1), 142–152.

Zou, W. W., & Xu, S. P. (2018). Galangin inhibits the cell progression and induces cell apoptosis through activating PTEN and caspase-3 pathways in retinoblastoma. *Biomedicine & Pharmacotherapy*, *97*, 851–863.

How to cite this article: Geng W, Ren J, Shi H, et al. RPL41 sensitizes retinoblastoma cells to chemotherapeutic drugs via ATF4 degradation. *J Cell Physiol*. 2020;1–12.
https://doi.org/10.1002/jcp.30010